

# Adaptive DFT-based fringe tracking and prediction at IOTA

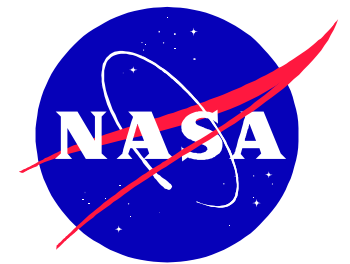
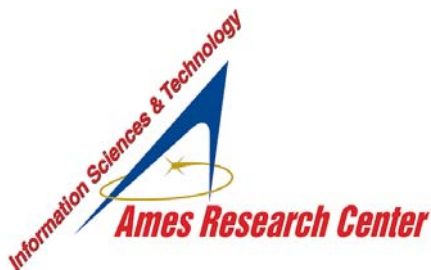
Edward Wilson (Intellization/NASA Ames),  
Ed.Wilson@intellization.com

Ettore Pedretti (U. Michigan / CfA)

Jesse Bregman (NASA Ames)

Robert W. Mah (NASA Ames)

Wesley A. Traub (Harvard-Smithsonian CfA)



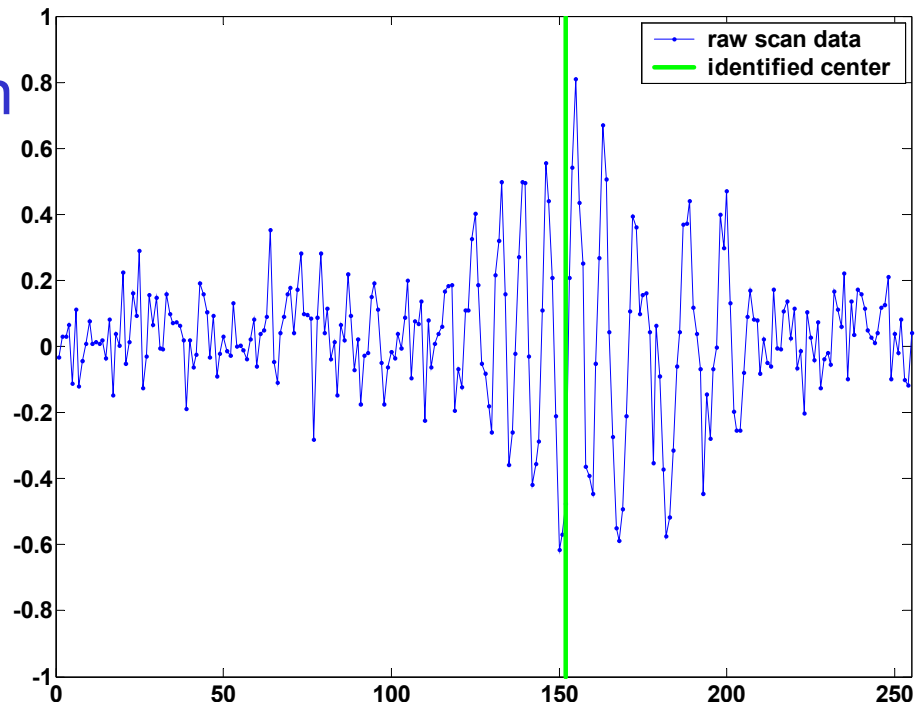
**Intellization**  
INTELLIGENT SYSTEMS FOR OPTIMIZATION

# Research overview

**Objective:** Develop and implement technologies to identify interferometric fringe packets in real-time for use in an automated fringe tracking system. Further, to develop neural-network based algorithms to predict fringe-packet motion to enable better tracking.

## Outline:

- Fringe packet identification
- Original algorithm
- Refined algorithm and implementation at IOTA
- Motion prediction
- Summary and future research



# Abstract

---

- An automatic fringe tracking system has been developed and implemented at the Infrared Optical Telescope Array (IOTA). In testing during May 2002, the system successfully minimized the optical path differences (OPDs) for all three baselines at IOTA. Based on sliding window discrete Fourier transform (DFT) calculations that were optimized for computational efficiency and robustness to atmospheric disturbances, the algorithm has also been tested extensively on off-line data. Implemented in ANSI C on the 266 MHz PowerPC processor running the VxWorks real-time operating system, the algorithm runs in approximately 2.0 milliseconds per scan (including all three interferograms), using the science camera and piezo scanners to measure and correct the OPDs. Preliminary analysis on an extension of this algorithm indicates a potential for predictive tracking, although at present, real-time implementation of this extension would require significantly more computational capacity.
- The system was developed off-line using actual data from IOTA, and was implemented and refined in 2002. The algorithms identify the center of a fringe packet by fitting a parametric model to the data. The results enable real-time fringe tracking, which is essential for phase closure among the three apertures. Accuracy of the algorithm output appears to be within the accuracy to which the true output is known.
- The fringe packet motion prediction system uses characteristics of past fringe packets to predict fringe packet motion. Initial investigations in this area have been done off-line. Fringe packet prediction, currently performed using an adaptive linear predictor, delivers 5-10% improvement over the baseline of predicting no motion.

# Timeline

---

- **[1998-1999]** 4000-scan data set from IOTA was used to develop the initial fringe tracking algorithm. Implementation not possible due to scanning hardware/communications limitations.
- **[Feb 2002]** Initial implementation of simplified and refined fringe tracking at IOTA. Unable to test on sky due to equipment/visibility problems.
- **[May 2002]** Successful implementation, some algorithm refinements to improve performance (tuning for characteristics of the new instruments).
- **[May 2004]** Successfully tested off-line on latest IOTA data.

# Fringe-packet identification

To enable on-line tracking and prediction, the first step is to autonomously identify the center of a fringe packet. The approach taken here was to fit the raw data to a parametric model representing a distortion-free fringe packet. The parametric model chosen was:

$$y = A \operatorname{sinc}(B(t+C)) \cos(D(t+E))$$

where  $y$  is the normalized value from the interferometer ((channelA-channelB)/(channelA+channelB)) and  $t$  is time. This particular grouping of parameters (e.g.,  $D(t+E)$  instead of  $Dt + E$ ) was chosen to facilitate gradient-based optimization of the functional parameters.

A combination of linear regression, gradient-based optimization, and fast Fourier transform (FFT) tools was used in designing the parameter identification algorithm.

The center of the fringe packet is represented by parameter  $C$ , and is the only one needed for simple fringe tracking. For prediction of fringe motion (and possible extensions, including on-line data reduction), all 5 parameters may be useful.

# Identification on IOTA data (original approach)

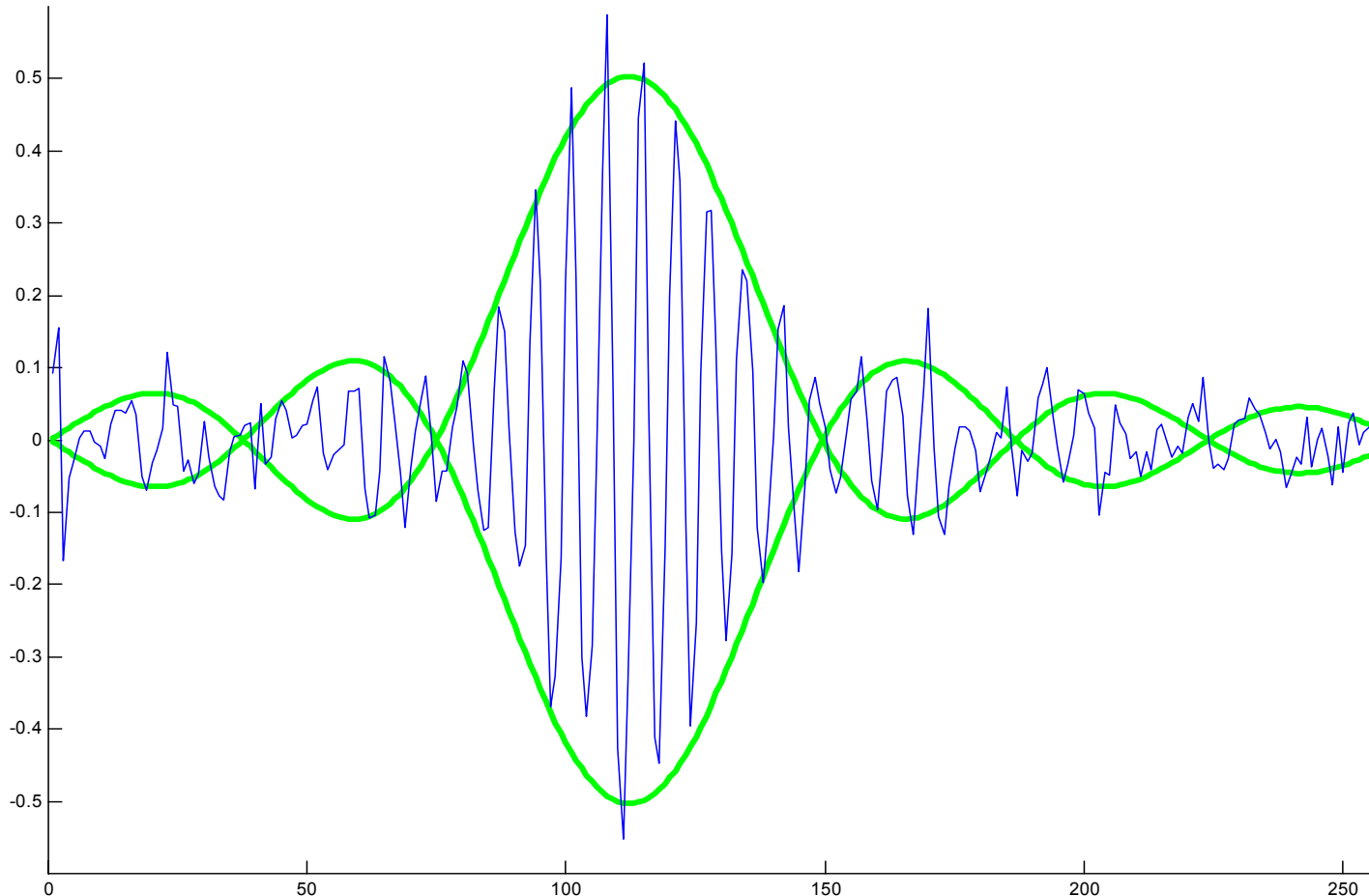
---

- Fringe packet parameters were identified on the 4000-scan data set from IOTA (1997 data) to an accuracy as good as can be determined by eye.
- That is, we can find fringe packet parameters (amplitude - **A**, spread of sinc function - **B**, center - **C**, frequency of fringes - **D**, and phase shift of fringes - **E**) that appear to be the “best” match to the actual data.

$$y = A \operatorname{sinc}(B(t+C)) \cos(D(t+E))$$

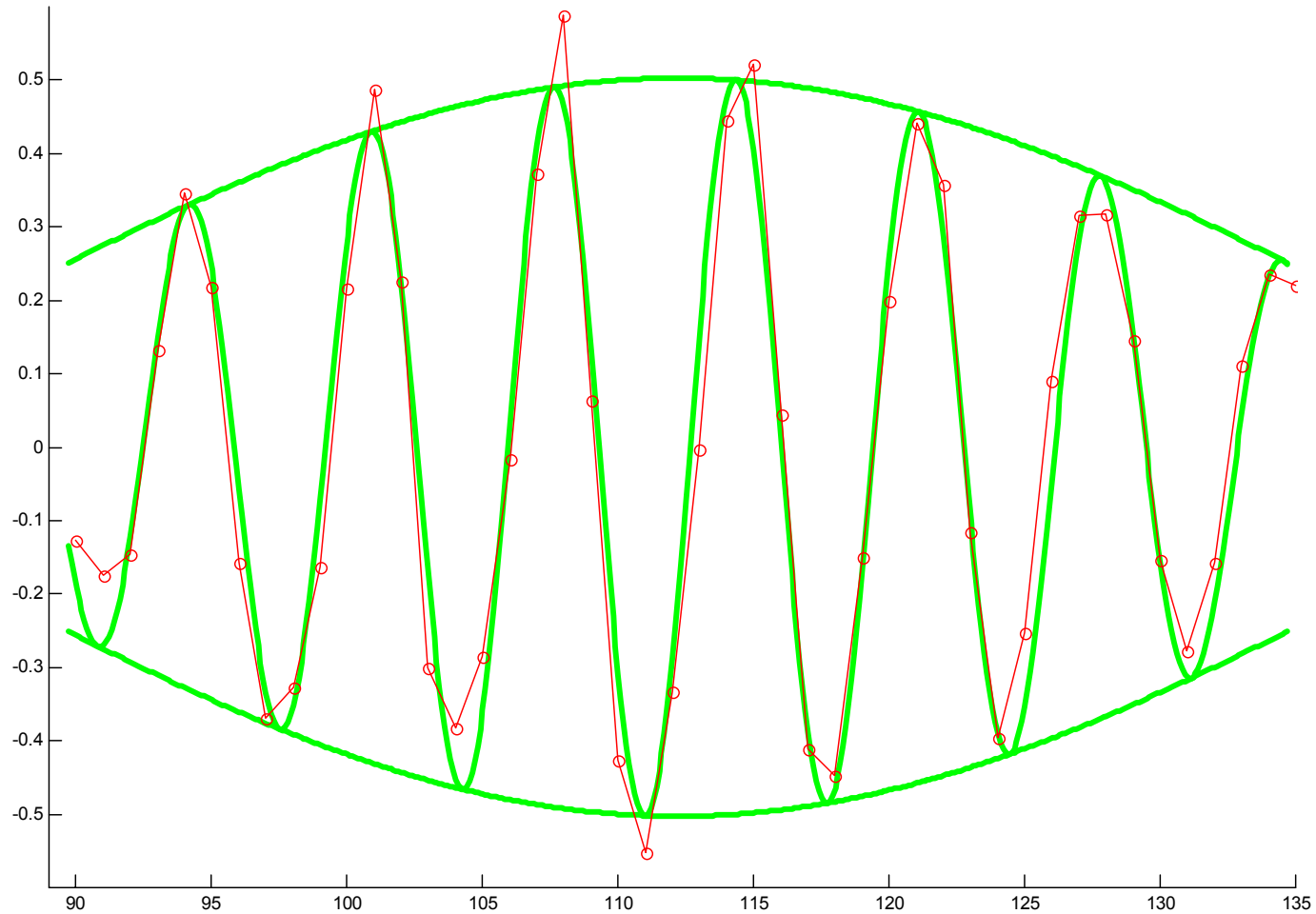
- Shown in the following two figures is an example of fitting to some data from IOTA.

# Envelope around raw data



Superposition of  $y = \pm A \text{ sinc}(B(t+C))$  with the actual data (data is discrete - one scan contains 256 points, but points have been connected to improve data visualization).

# Fit to packet center



Zoomed in on the packet center, also showing superposition of the full function,  $y = A \text{sinc}(B(t+C)) \cos(D(t+E))$ .

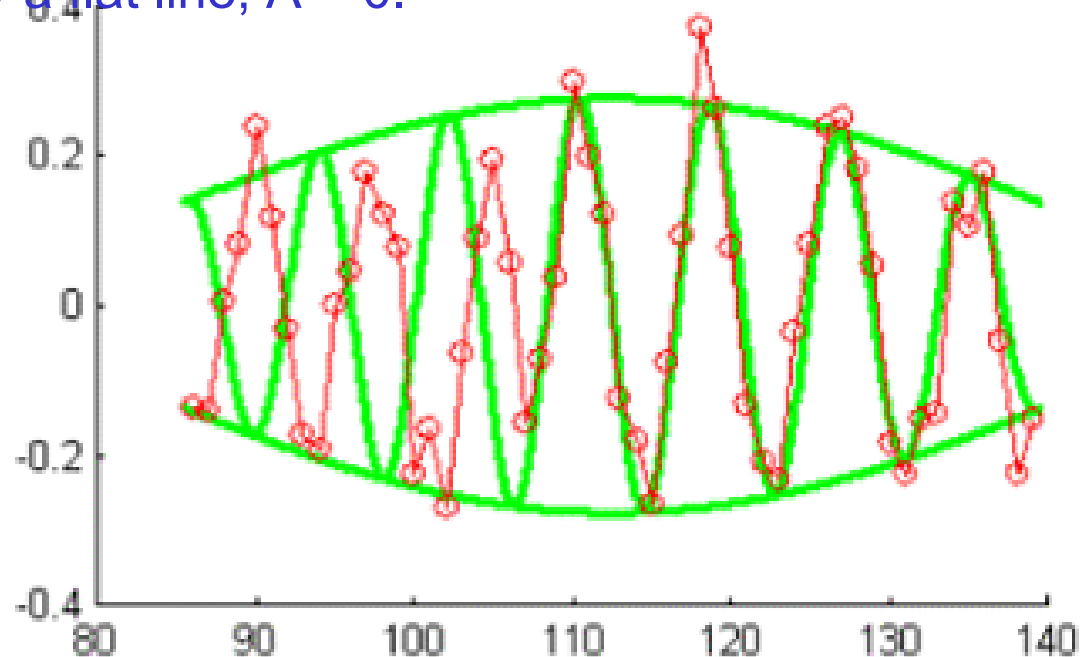
# Original algorithm

Summary of the steps in identification (original algorithm):

- 1) Data sets from each of the two collectors are combined:  $y = (\text{channelA} - \text{channelB}) / (\text{channelA} + \text{channelB})$
- 2) Outliers and local bias are removed
- 3) Envelope of the absolute value of the signal is calculated, eliminating the individual fringes. Ideally this function would be  $y = A \text{ abs}(\text{sinc}(B(t+C)))$
- 4) An estimate for the center of the fringe packet (C) is found by maximizing weighted symmetry over the envelope.
- 5) Using an initial guess for B, the remaining parameter A is found by a least squares fit to the data.
- 6) Now that A, B, and C have good initial estimates, a gradient-based optimization is performed to find A, B, and C that form the least squares fit to the data.
- 7) Fringe parameters, D and E, are found by fitting the ideal fringe function to the data over the center of the fringe packet (half height of the sinc function determines the center region).
- 8) FFT provides an initial guess for D and E, and a gradient-based optimization finds C, D and E, with A and B held fixed.

# Intra-packet phase shift

- Simultaneous gradient-based optimization of A, B, C, D, and E did not work as well on the noisy data as the sequential procedure listed above. One example of a reason for this difficulty can be seen here: half-way through the fringe-packet scan, a sudden phase shift was encountered.
- If all 5 parameters were adapted simultaneously, the result would be a flat line, with  $A=0$ , since the identification would be unable to lock onto the left and right halves of the fringe packet. Squared error would be minimized approximately by a flat line,  $A = 0$ .
- With sequential ID, A and B, representing the sinc function envelope, were held fixed while the fringe frequency and phase shift (D and E) were identified. The ID locked onto the right half of the fringe packet.

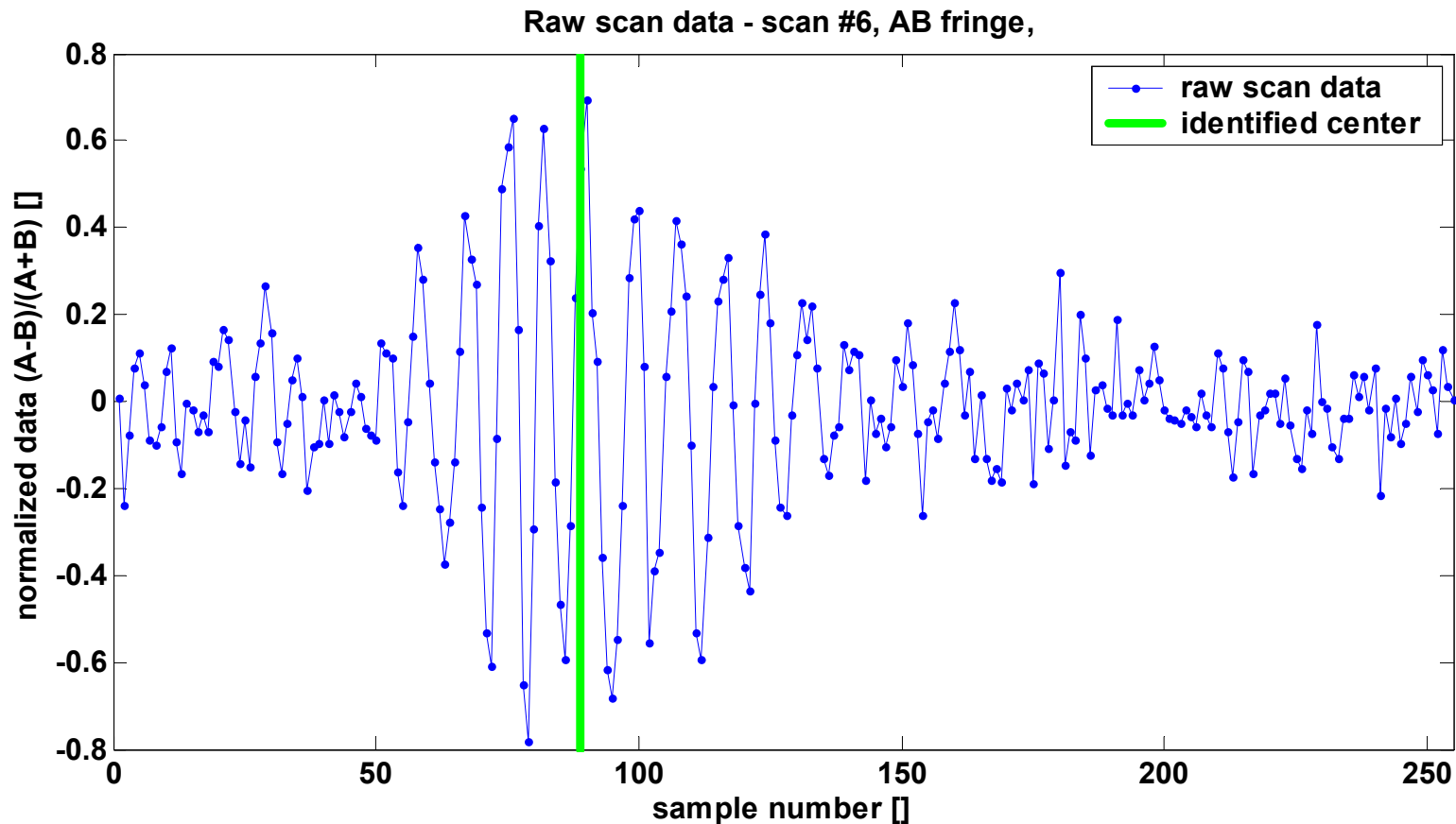


# Implementation, refined algorithm

---

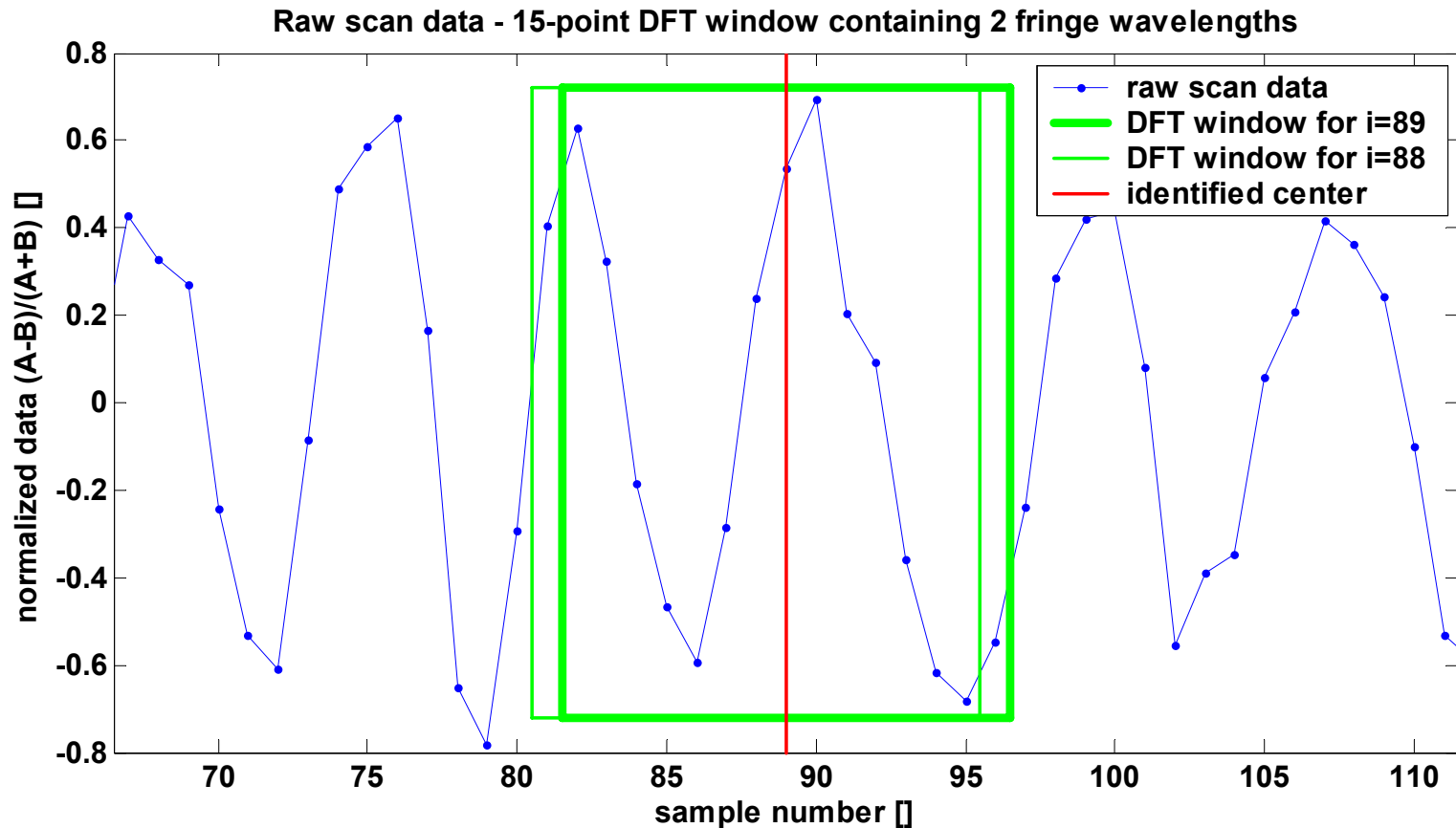
- The original algorithm was improved (DFT-based rather than envelope-based), and in 2002 was ported to ANSI C for implementation on the real-time tracker at IOTA.
- When data from all 3 apertures and the new collection instruments became available, further tuning was performed.
- Tracking ran successfully, enabling phase closure on the three apertures. Computation takes 2.0 milliseconds per scan (for all three interferograms) on the real-time PowerPC processor (VxWorks RTOS).
- The C source code (and equivalent MATLAB code) has been delivered to IOTA.

# Raw data



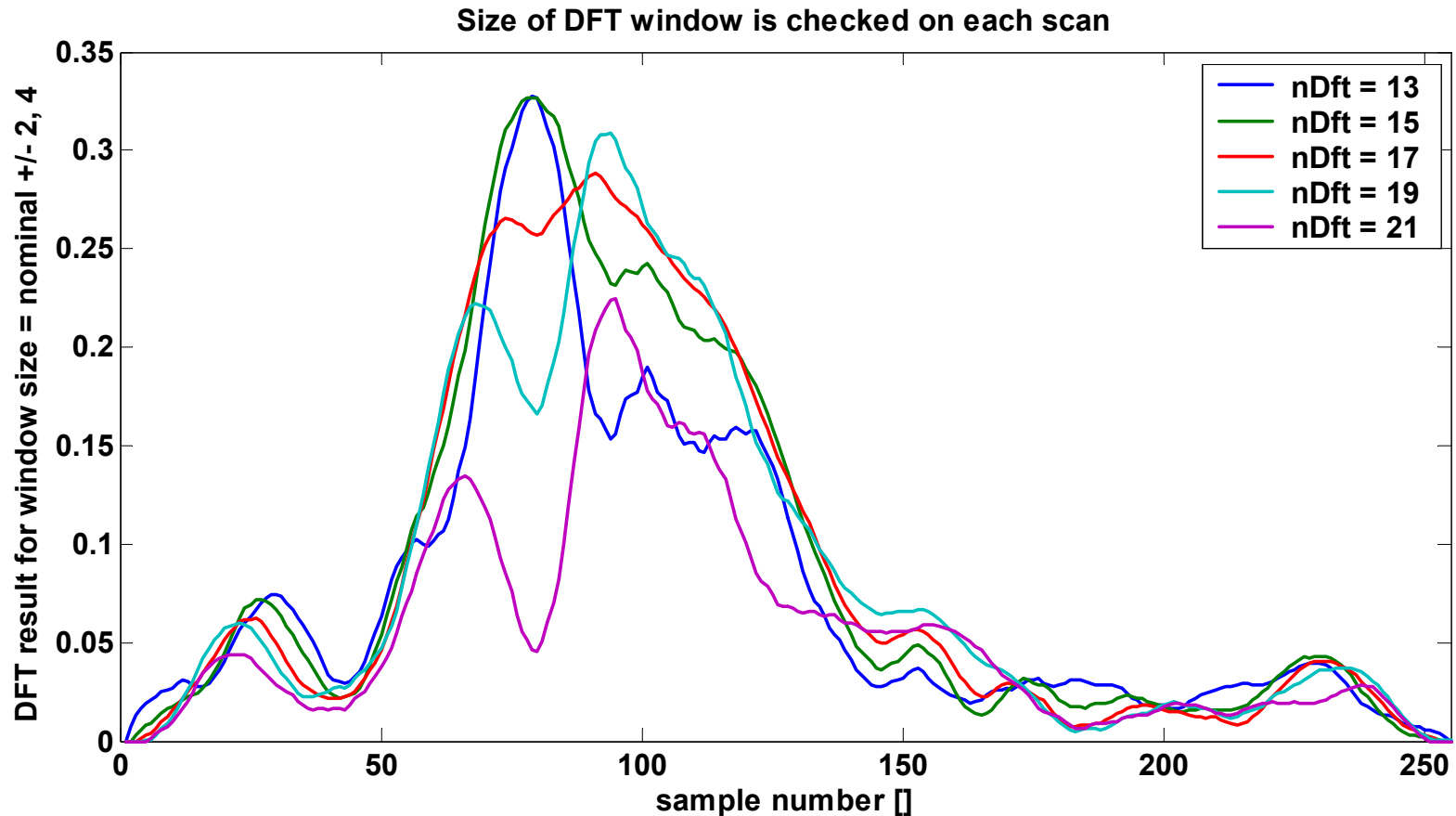
Raw data (combined using  $(A-B)/(A+B)$ ), as well as the result of the center identification that came after all steps were completed

# DFT window scanned over data



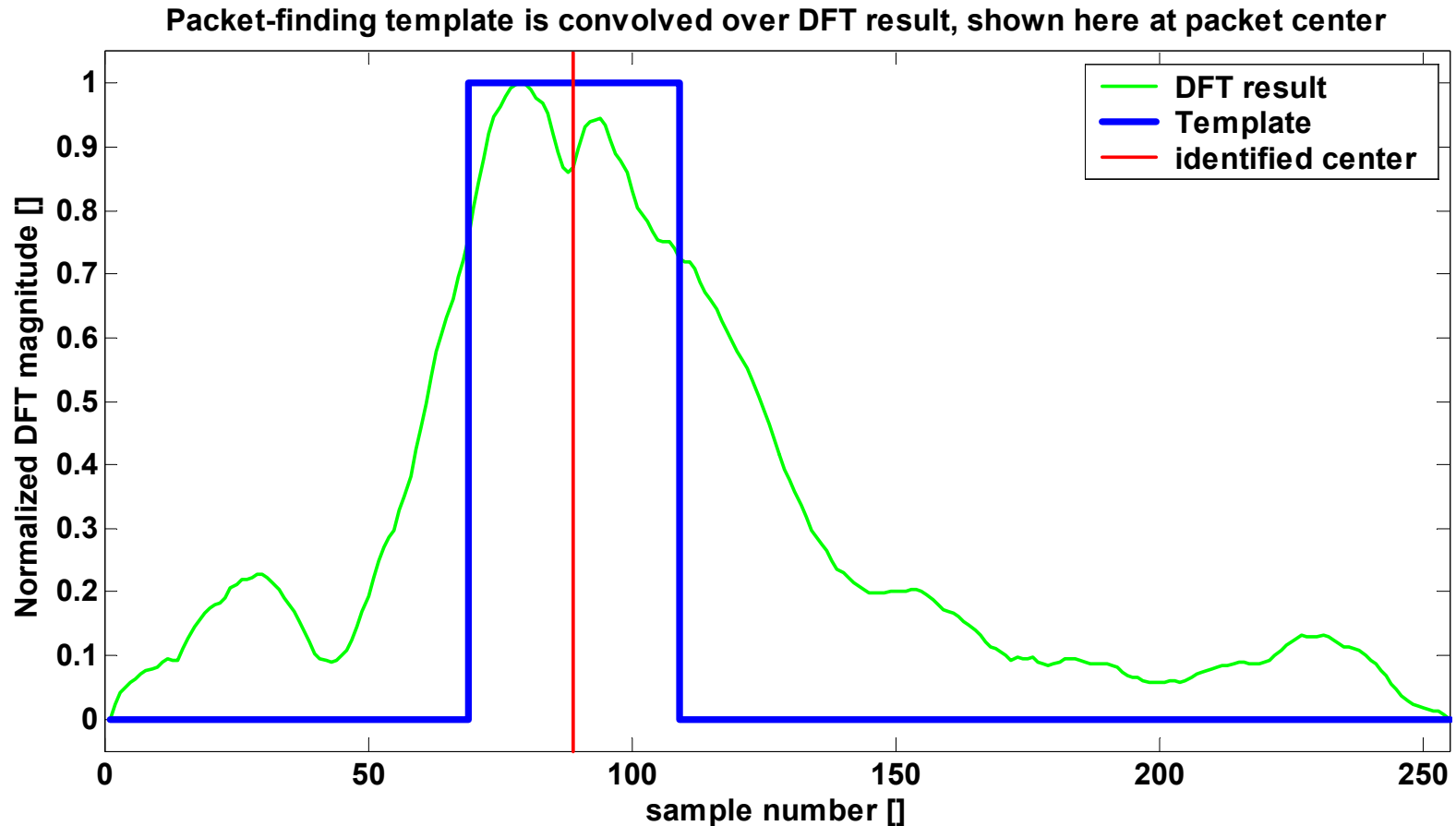
DFT window is passed over the raw data, locating areas in the scan where the expected fringe frequency is present. DFT computation by a customized algorithm to optimize efficiency.

# Smoothed DFT results for range of DFT window sizes



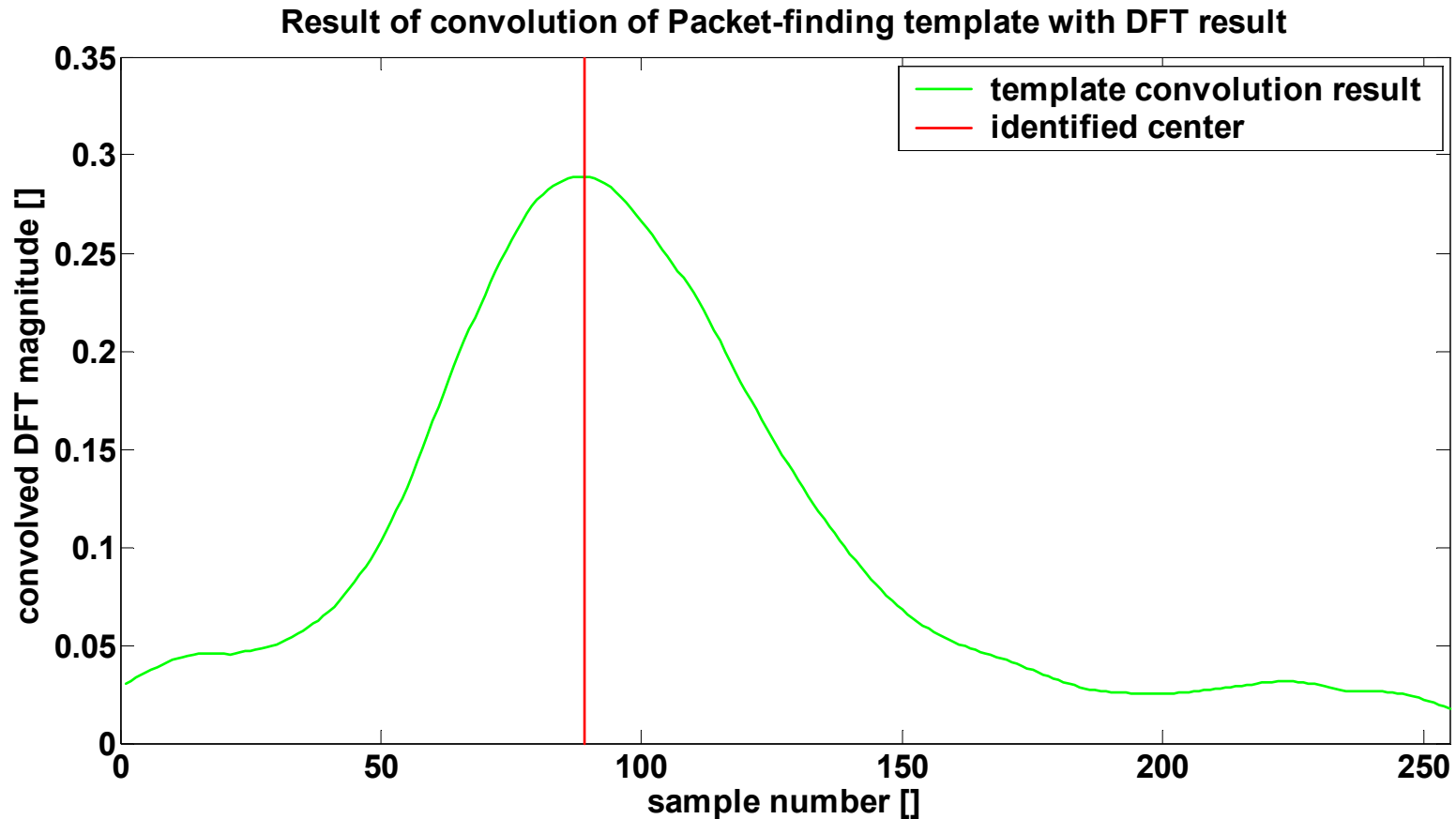
- The DFT results are smoothed with an averaging window passed over the data. This step is computationally efficient, and reduces the variability in the DFT results.
- Use of multiple window sizes increases robustness to intra-packet fringe frequency variation, and enables adaptation to the fringe frequency.

# Convolution of combined DFT results with packet template



The maximum result from the 5 DFTs is taken (green line here), then a rectangular packet-finding template is passed over that result.

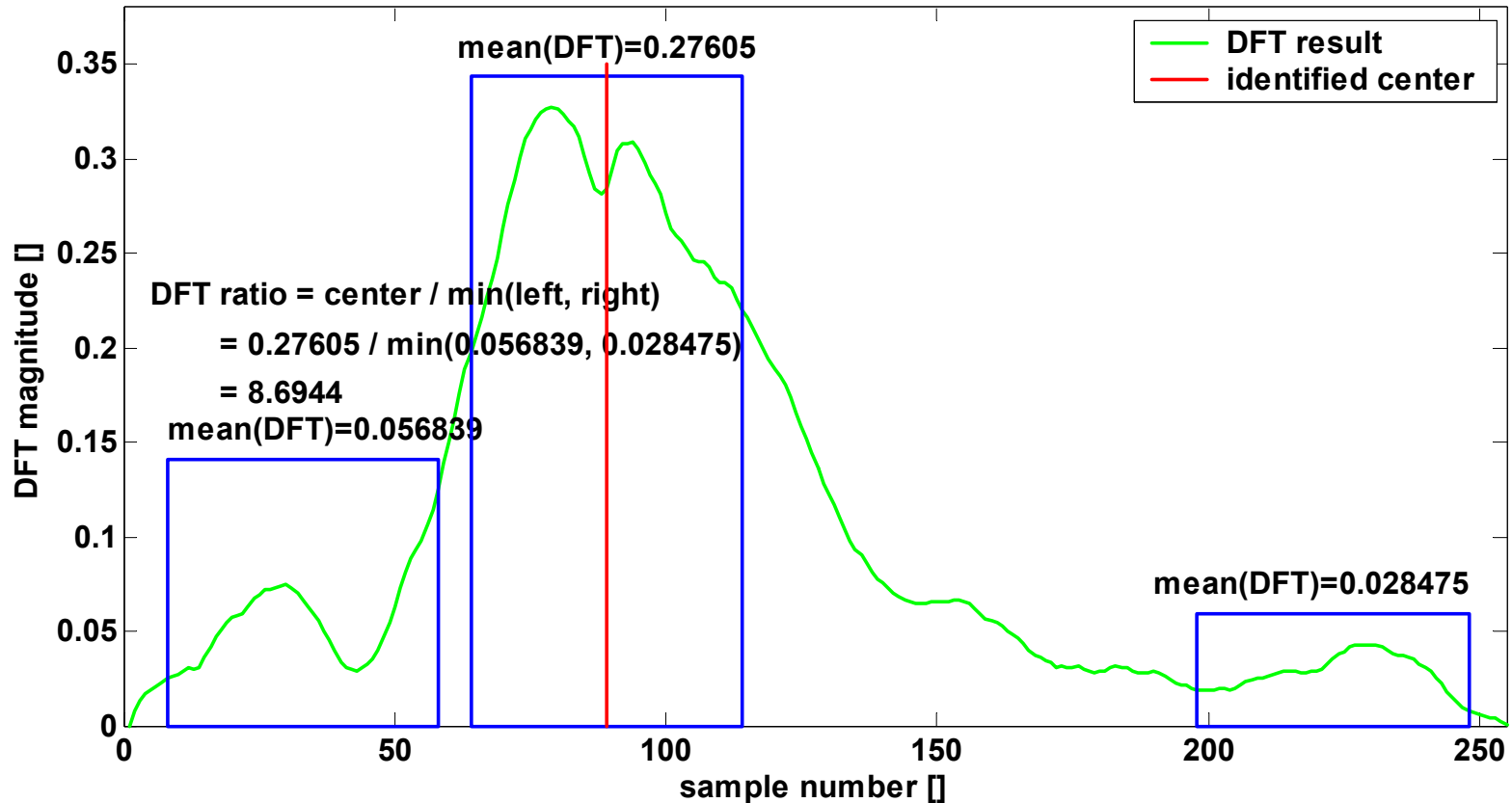
# Convolution result



Result of convolution is shown. Index corresponding to maximum value is taken as the identified result.

# Confidence metric

Calculation of confidence metric, dft\_ratio = 8.6944



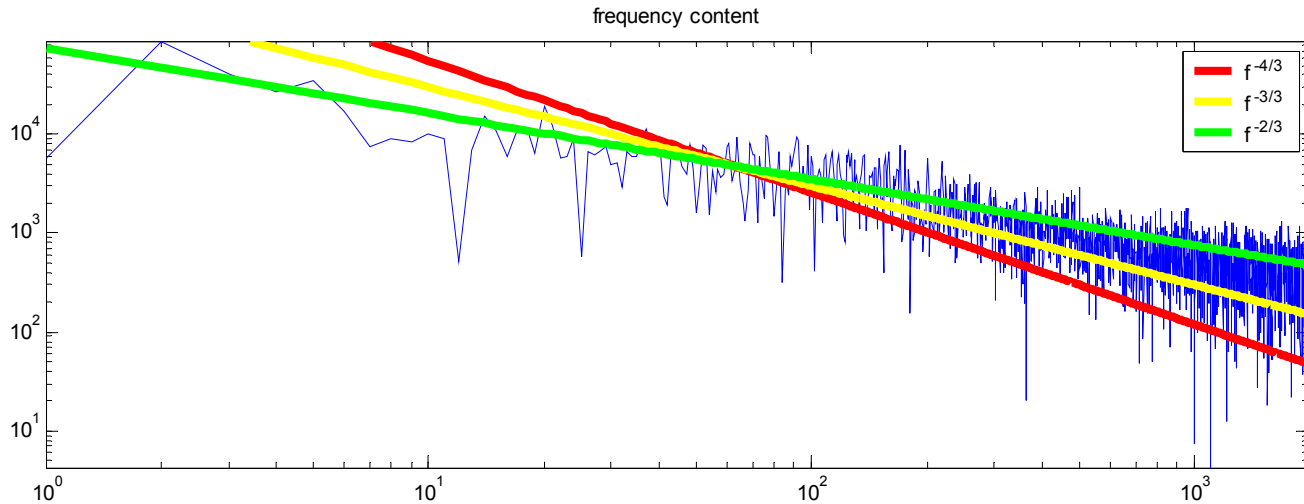
Confidence metric calculated based on DFT results at packet center and both scan ends. Confidence measures from each of 3 interferograms weight the ID results' influence in centering the next scans.

# Fringe Motion Prediction

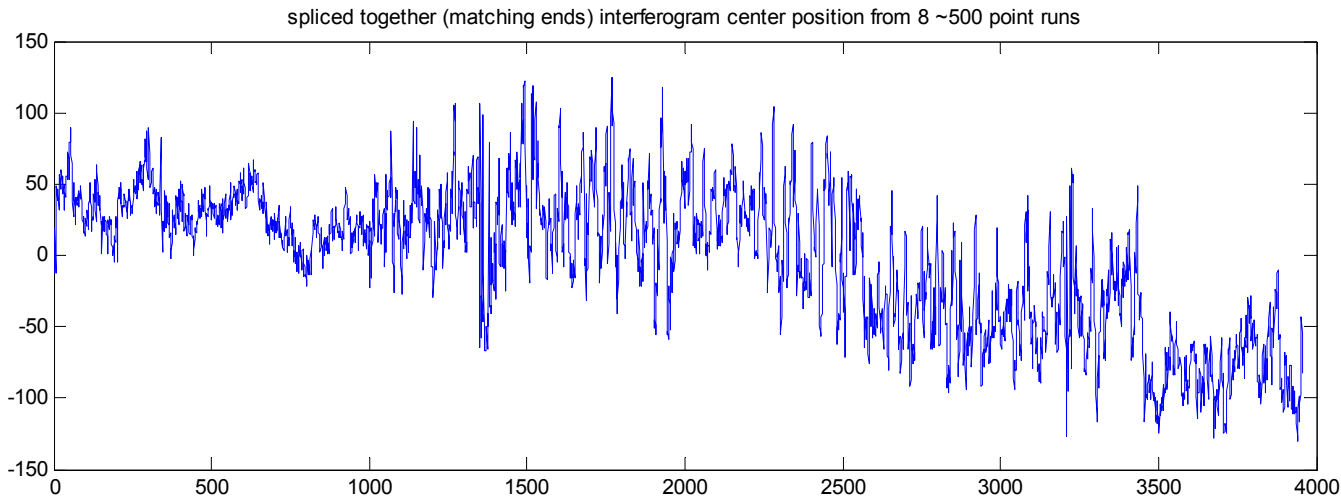
---

- Initial experiments with fringe packet motion prediction were performed as a proof of concept.
- Since fringe motion is based on atmospheric changes, and these changes are not completely random (noise spectrum is proportional to frequency  $^{\wedge} (-2/3)$  rather than white noise), there should be some component of motion that is predictable.
- An adaptive linear model using present and past identified fringe parameters was developed as a first step. The center of the next fringe packet and the magnitude of fringe-packet-center motion were predicted, with the goal of optimizing on-line the parameters (e.g., travel limits and rate) of the next scan.
- At best, this model produced approximately 10% improvement over no prediction (i.e., predicting that the fringe packet would remain where it was on the next scan). On average, the improvement was 5%. Extension to nonlinear prediction methods, including neural networks is under investigation.

# Fringe motion noise spectrum



- Spectrum is not white, indicating a predictable component
- Noise magnitude depends on target, atmospheric conditions
- $f^{-2/3}$  observed
- Analysis based on ID results from 1997 IOTA data (4000 scans)



# Prediction with adaptive linear model (proof of concept)

	col1	col2	col3	col4	col5	col6	col7	col8		[Mean]
Data set 0	7.507	7.854	7.765	6.521	3.889	6.680	4.097	6.489		6.350
<b>Data set 2</b>	<b>8.939</b>	<b>9.978</b>	<b>9.550</b>	<b>10.232</b>	<b>6.238</b>	<b>6.826</b>	<b>4.961</b>	<b>6.272</b>		<b>7.874</b>
Data set 3	5.267	4.787	4.717	4.959	-0.818	5.280	4.673	2.829		3.962
Data set 5	2.312	2.786	3.883	3.583	3.556	3.841	2.804	2.739		3.188
Data set 6	7.506	7.581	7.453	7.502	3.026	4.301	6.893	2.850		5.889
Data set 7	0.778	-0.149	0.836	1.832	0.637	1.790	2.566	-0.279		1.001
Data set 8	-0.102	2.864	3.118	3.067	-0.350	3.017	3.861	2.768		2.280
Data set10	0.841	2.403	0.890	0.880	0.511	1.954	0.674	1.270		1.178
Data set11	2.940	2.675	3.081	3.074	1.476	2.953	2.931	1.259		2.548
-----										
[Mean]	3.998	4.531	4.588	4.628	2.018	4.071	3.718	2.911		

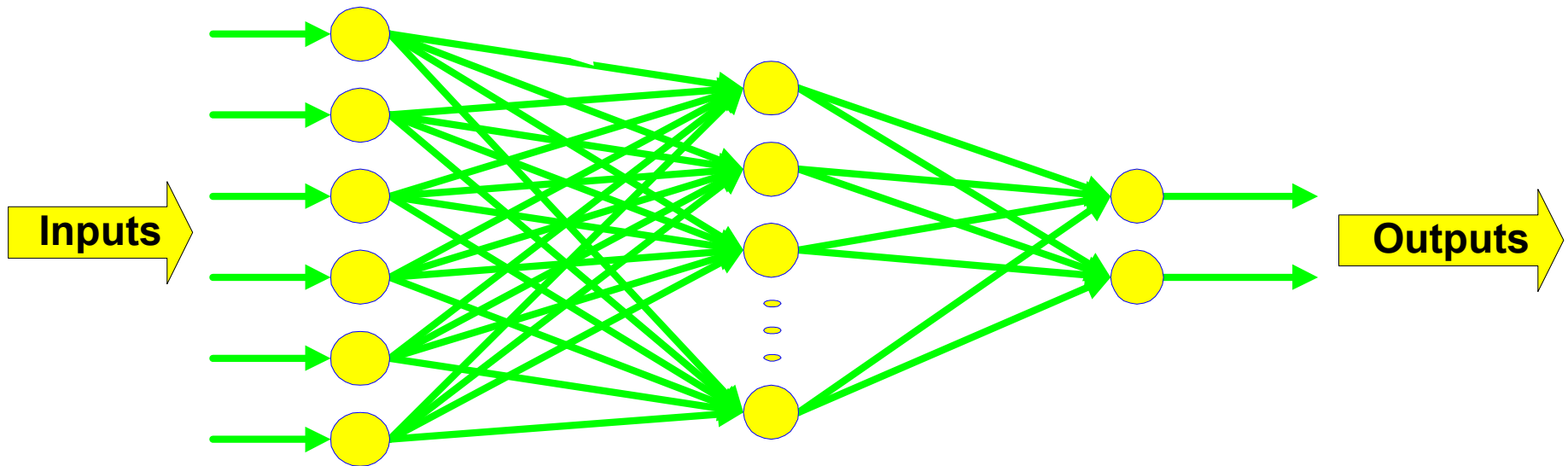
Variables used in prediction [y = A \* sinc(B(x+C)) .\* cos(D(x+E))]:

col 1 :	A	B	C	D	E	A_delta	B_delta	C_delta	D_delta	ones_n_1
col 2 :			C	D			B_delta	C_delta	D_delta	ones_n_1
col 3 :			C	D			B_delta	C_delta		ones_n_1
<b>col 4 :</b>			<b>C</b>	<b>D</b>				<b>C_delta</b>		<b>ones_n_1</b>
col 5 :				D				C_delta		ones_n_1
col 6 :			C					C_delta		ones_n_1
col 7 :			C	D						ones_n_1
col 8 :			C	D				C_delta		

- Least-squares linear predictors, various input variables tested
- Test/training data sets from 1997 IOTA data
- Baseline for comparison – predict no motion

# Neural Network Background

Neural network – signal processing technology inspired by and loosely modeled after the human brain



- Generic **nonlinear** functional element
- Functionality (defined by weights) set through *“training”* process
- Massively **parallel** architecture – can be implemented in hardware
- **Several applications** in industrial process control, credit scoring, fraud detection, target recognition, optical character recognition, etc.

# Other Publications

---

- “On-line fringe tracking and prediction at IOTA,” E. Wilson and R. Mah, in *Proceedings of the 18th Congress of the International Commission for Optics*, San Francisco, California, August 1999.
- “Fringe-tracking experiments at the IOTA interferometer,” S. Morel et al, Proc. SPIE 4006, 2000.
- “Fringe tracking at the IOTA interferometer,” E. Pedretti, et al, Proc. SPIE 5491-62, 2004.
- “Adaptive DFT-based interferometer fringe tracking,” E. Wilson, et al, in *EURASIP Journal on Applied Signal Processing – special issue on Applications of Signal Processing in Astrophysics and Cosmology*, Q2, 2005 (submitted).

# Summary of results

- Interferogram center ID works very well on all data sets tested (1997, May 2002, Apr 2004). The fringe-center estimate provided by the initial steps of the full algorithm appears to be sufficiently accurate for fringe tracking. That is, the initial estimate of  $C$  in the equation  $y = A \operatorname{sinc}(B(x+C)) \cos(D(x+E))$  is sufficient, and full nonlinear estimation of  $A$ ,  $B$ ,  $C$ ,  $D$ ,  $E$  provides only marginal improvement. The adaptive nature of the DFT-based algorithm virtually eliminates the need to set any target-dependent parameters, and provides robust tracking in the presence of significant atmospheric distortion.
- Implementation and refinement at IOTA was completed in May 2002, using all three telescopes. Compute time on the real-time PowerPC processor is 2.0 ms for all 3 interferograms. Accuracy is sufficient to enable phase closure, but no quantitative results have yet been derived from these tests.
- Modeling the effect of atmospheric turbulence was pursued in very early stages. This was to have been useful for control system development in simulation.
- Prediction of interferogram motion using adaptive linear predictors appears feasible, but the additional payoff appears small relative to that achieved through fringe tracking control (without prediction).

# Acknowledgements

---

- The algorithm development work presented here was funded through Director's Discretionary Fund awards at NASA Ames Research Center.
- The authors wish to thank the staff and other researchers at IOTA for their invaluable contributions to the research facility.
- The IOTA is operated by the Smithsonian Astrophysical Observatory, a member of the Harvard-Smithsonian Center for Astrophysics.